

## ORIGINAL ARTICLE

# Sensory Deviancy Detection Measured Directly Within the Human Nucleus Accumbens

Stefan Dürschmid<sup>1,3,4</sup>, Tino Zaehle<sup>3,4,5</sup>, Hermann Hinrichs<sup>3,4,6,7</sup>, Hans-Jochen Heinze<sup>3,4,6,7</sup>, Jürgen Voges<sup>5,6</sup>, Marta I. Garrido<sup>8,9,10</sup>, Raymond J. Dolan<sup>11,12,13</sup>, and Robert T. Knight<sup>1,2</sup>

<sup>1</sup>Helen Wills Neuroscience Institute, <sup>2</sup>Department of Psychology, University of California, Berkeley, CA, USA, <sup>3</sup>Department of Behavioral Neurology, Leibniz Institute of Neurobiology, Magdeburg, Germany, <sup>4</sup>Department of Neurology, <sup>5</sup>Department of Stereotactic Neurosurgery, Otto-von-Guericke University, Magdeburg, Germany, <sup>6</sup>German Center for Neurodegenerative Diseases (DZNE), Magdeburg, Germany, <sup>7</sup>Forschungscampus STIMULATE, <sup>8</sup>Queensland Brain Institute, <sup>9</sup>Centre for Advanced Imaging, <sup>10</sup>Australian Research Council Centre of Excellence for Integrative Brain Function, The University of Queensland, Brisbane St Lucia, QLD 4072, Australia, <sup>11</sup>Wellcome Trust Centre for Neuroimaging, UCL, London, UK, <sup>12</sup>Visiting Einstein Fellow, Humboldt University Berlin, Berlin, Germany, and <sup>13</sup>Max Planck UCL Centre for Computational Psychiatry and Ageing Research, London, UK

Address correspondence to Stefan Dürschmid. Email: stefan.duerschmid@googlemail.com

## Abstract

Rapid changes in the environment evoke a comparison between expectancy and actual outcome to inform optimal subsequent behavior. The nucleus accumbens (NAcc), a key interface between the hippocampus and neocortical regions, is a candidate region for mediating this comparison. Here, we report event-related potentials obtained from the NAcc using direct intracranial recordings in 5 human participants while they listened to trains of auditory stimuli differing in their degree of deviation from repetitive background stimuli. NAcc recordings revealed an early mismatch signal (50–220 ms) in response to all deviants. NAcc activity in this time window was also sensitive to the statistics of stimulus deviancy, with larger amplitudes as a function of the level of deviancy. Importantly, this NAcc mismatch signal also predicted generation of longer latency scalp potentials (300–400 ms). The results provide direct human evidence that the NAcc is a key component of a network engaged in encoding statistics of the sensory environment.

**Key words:** auditory mismatch, P3, prediction error, predictive coding, nucleus accumbens, saliency

## Introduction

The ability to detect unexpected environmental events is a fundamental property of organized mammalian behavior (Kane et al. 1993, 1996). This capacity depends on a comparison of the actual state of our sensory world with predictions based on immediate and long-term contextual knowledge. Predictive coding theory, first articulated within the visual domain, postulates that neural networks learn statistical regularities of the natural world,

signaling deviations from these regularities to higher centers in order to guide behavior (Rao and Ballard 1999). This allows predictable components of an input signal to be removed and redundancy reduced. At a neurophysiological level, it has been suggested that backward connection strength is increased, and forward connections decreased, with temporal regularities (Kumar et al. 2011) so as to establish stable sensory memory representations when no prediction error (PE) signals occur.

One subcortical region implicated in the expression of PEs is the nucleus accumbens (NAcc), a region implicated in goal-directed behavior (Goto and Grace 2008) and known to be sensitive to novelty (Wood et al. 2004), contextual deviance (Axmacher et al. 2010), aversive stimuli (Becerra et al. 2001; Baliki et al. 2010), and reward PEs in humans (Abler et al. 2006; Spicer et al. 2007). These findings indicate that the NAcc may serve as a critical hub in deviancy detection. However, the neural underpinnings engaged in the human NAcc during deviancy detection and generation of sensory PEs are unknown.

We recorded directly from the NAcc in 5 human subjects participating in an experiment (Garrido et al. 2008), permitting detailed analysis of gradual strengths of sensory mismatch and expectancy. We predicted that the NAcc would weight how new information fits into an ongoing sensory context and convey information about this deviation to regions in the cortical hierarchy. This led us to hypothesize that (1) the NAcc would generate a sensory-evoked mismatch signal, (2) that this mismatch signal should vary as a function of deviance strength, and (3) that a NAcc mismatch response would contribute to the later onset of cortical mismatch components involved in behavioral adjustments. Here, we provide intracranial and simultaneous scalp electroencephalographic (EEG) data that show NAcc signals the strength of a PE during perception of auditory regularities and this PE predicts later cortical activity.

## Methods

Five patients (mean  $\pm$  SD age: 40  $\pm$  9.02 years; 3 males/4 females, all right-handed) with a history of intractable epilepsy participated in this study. We recorded intracranially from bilateral NAcc (Fig. 1A) and bilateral anterior thalamus (ANT). We also recorded from electrodes positioned at midline scalp sites. For details on surgery, deep brain stimulation approach, and placement of surface electrodes see Zaehle et al. (2013).

## Paradigm

We employed a paradigm requiring passive listening to a sequence of sine wave sounds (tone pips) with an interstimulus interval of 0.5 s and constant loudness (Fig. 1B; Garrido et al. 2008). The frequency of sounds varied across 7 different levels between 500 and 800 Hz with increments of 50 Hz. Sounds of

the same frequency formed a train and train length was defined by the number of repetitions of the initial sound. The number of repetitions ranged between 0 and 10 (Fig. 1). The first sound with a frequency other than the previous train was defined as a deviant sound. This sound along with its next  $N$  repetitions formed the next train. To prevent an onset clicking sound for the stimuli, a 10-ms sigmoid ramp was applied to the on- and offset of each sound. Each sound was presented for 70 ms. Participants were presented with either 1800 (Pat01/Pat02: 15 min) or 1200 trials (Pat03/Pat04/Pat05: 10 min).

## Stimulus Repetition

The number of repetitions ( $N_{\text{rep}}$ ) varied between 0 and 10. In the case of 0 repetitions, a deviant stimulus was followed by another deviant stimulus. In the case of 10 repetitions, the deviant stimulus was followed by 10 standards (resulting in 11 sounds of the same tone pitch in a train; Fig. 1C). The probability of  $N_{\text{rep}} \geq 5$  was 87.5% compared with  $N_{\text{rep}} < 5 = 12.5%$  to assure that deviant stimuli were perceived as rare events (Fig. 1C). To compare deviant trials as a function of the train length, we chose the same probability of trains with  $N_{\text{rep}} \geq 5$  to equate the number of deviant trials. Sequences of  $N_{\text{rep}}$  were randomly presented throughout the experiment independent of the frequency of the sounds. This means that a 500-Hz sound could be repeated by 0–10 500 Hz sounds as well as an 800-Hz sound or all other sounds of the 7 pitch levels. Hence, sound pitch and  $N_{\text{rep}}$  of the following sound were unpredictable. The probability of a deviant stimulus was approximately 15%.

## Deviation Strength

The absolute deviation strength (DS) varied with 6 levels of DS. The strongest deviation was 300 Hz (i.e., 500–800 or 800–500 Hz), and the weakest deviation was defined as a 50-Hz change (i.e., 500–550 or 700–650 Hz; Fig. 1B).

## Data Collection

Intracranial recordings were obtained using a Walter Graphtek (Walter Graphtek GmbH, Lübeck, Germany) system, with a sampling rate of 256 Hz and analog bandwidth of 200 Hz. In the left and right NAcc and ANT, adjacent electrodes were referenced to the neighboring contact (i.e., 1–2, 2–3, 3–4, with “1”

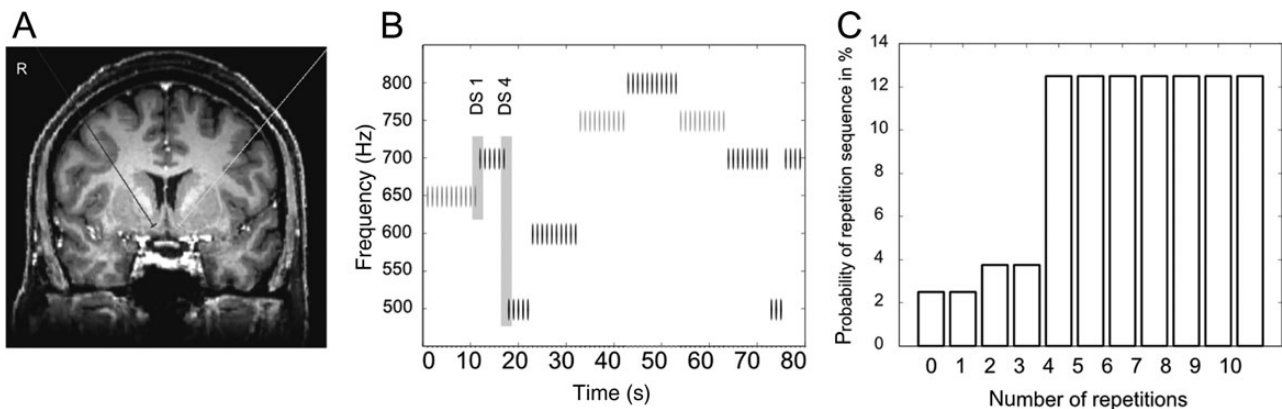


**Figure 1.** Depiction of the roving paradigm. (A) Anatomical location of bilateral NAcc depth electrodes. (B) Seven different sound levels were defined differing only with respect to their frequency (500–800 Hz). Each sound as indicated by the grayscale vertical lines was presented with a random number of repetitions, which were independent of the frequency of the sound. The difference in tone pitch between the standards and the deviant sound defined the DS. (C) The number of repetitions varied between 0 and 10.

representing the most ventral and “4” representing the most dorsal electrode contact). This resulted in a bipolar montage with each NAcc/ANT monitored by 3 electrode positions. This montage was used to enhance the spatial resolution of the intracranial recordings and to ensure that the recorded activity was not due to far-field activity from nearby non-NAcc structures.

### General Data Analysis

We used Matlab 2009b (Mathworks, Natick, MA, USA) for all off-line data processing. The resulting time series for the electrodes located in the NAcc were segmented in epochs of  $-1$  to  $2$  s relative to the event (stimulus onset). We filtered the resulting epochs applying a bandpass filter between  $0.1$  and  $20$  Hz. All filtering was done using a fourth-order Butterworth filter (IIR-filters). To exclude trials affected by artifacts, we defined a threshold for the exclusion of trials in each analysis. In each trial  $t$ , we calculated the variance of the bandpass filtered activity across the epoch. All trials exceeding  $2$  SD above the mean variance were excluded from analysis.

We tested the hypotheses that a response in the NAcc (1) differentiates between standard and deviant stimuli and (2) represents the strength of deviation. In addition, we hypothesized (3) that the NAcc capacity to signal deviation depends on the strength of recent memory so that small deviations are better signaled if a memory trace is well established. Finally, the most prominent component of novelty is the fronto-parietal P300 response dependent on frontal-hippocampal regions in humans (Knight 1996; Knight and Scabini 1998; Boly et al. 2011). Thus, (4) we also predicted that a NAcc computation of a PE would drive a scalp P300 response. In each analysis, we compared the statistical parameters with an empirical distribution derived from a permutation procedure. In that procedure, all baseline-corrected epochs comprising the trial duration ( $0$ – $500$  ms) were randomly shifted in time. All epochs both of each trial and of each subject were shifted independently. In temporal intervals exceeding the 95% confidence interval (CI), we also report the minimal  $P$ -value within the empirical distribution.

### Coding of the PE

The mismatch signal is defined as the difference in the event-related activity between standard and deviant stimulus-related potentials. To measure this we calculated the event-related potential for both standard and deviant stimuli for each subject. For both stimulus types, we averaged across all intracranial recording sites and trials. The evoked responses of the 4th to the last (10th) standard in a train were assigned to the set of standard trials to equate for the number of trials for standards and deviants. For each epoch, we subtracted the baseline activity ( $-500$  to  $0$  ms before the stimulus onset) and calculated the  $t$ -value using a paired  $t$ -test for each time point. The resulting  $t$ -value time series represents the strength of difference between standard and deviant stimuli across participants as a function of time. The statistical significance of each  $t$ -value was assessed by comparing the  $t$ -values with an empirical distribution derived from a permutation procedure (Blair and Karniski 1993). All epochs were randomly shifted in time, and the shifted epochs were averaged and the  $t$ -values between standard and deviant stimuli were calculated for each time point exactly as for the observed time series. This permutation procedure was repeated 500 times. For each time point, the CIs (2.5% and 97.5%) of a normal distribution were determined. All  $P$ -values reported show the probability of the observed  $t$ -value within the distribution derived from the permutation procedure.

### PE Depending on Deviation Strength

Throughout the experiment, we randomly varied the DS and the number of standards. We directly tested the gradual deviancy variation with a linear regression and grouped trials associated with deviant stimuli according to the absolute strength of deviation to assess a gradual variation in the DS. Here, the strength of deviation is defined as the difference in frequency between each deviant sound and the preceding standard sound. We used deviant sounds following trains of 5–11 sounds, meaning deviants following the 4th to the 10th standard (corresponding to the same set of trains as in the section “Coding of the PE”). Six different groups of DS were classified ranging from DS = 50 Hz (e.g., 500–550 or 700–650 Hz) to DS = 300 Hz (500–800 or 800–500 Hz). We averaged across trials within each deviation group. This results in 6 time series per subject each 1 trial long. Using linear regression, we tested the hypothesis that differences in DS predict differences in recorded amplitude. For each point in time, we estimated the linear equation

$$\hat{y} = a \times x + b$$

with the vector  $x$  as the 6 amplitude values,  $\hat{y}$  as the predicted DS,  $a$  as the slope parameter, and  $b$  as the intercept. The individual slope parameters were averaged across participants and the averaged slope parameters were used to determine the temporal intervals in which differences in amplitude predict differences in DS. The slope parameter is positively/negatively high if a stronger deviation elicits greater amplitude values in a given temporal interval. To assess significance, we performed a permutation procedure with 500 runs in which the same linear regression analysis was conducted with randomly shifted time series. All epochs were shifted in time separately. The shifted epochs were averaged and the slope values were calculated for each time point exactly as for the observed time series. For each time point, the CIs (2.5% and 97.5%) of a normal distribution were determined. Time points with the slope parameter  $a$  exceeding the CI were considered significant. Reported  $P$ -values show the probability of the observed slope value within the distribution derived from the permutation procedure.

### PE Depending on Auditory Regularity

We hypothesized that sensitivity to deviant stimuli with only a small DS varies as a function of the number of preceding standard sounds (Haenschel et al. 2005). We tested whether a mismatch of small DS following a long train elicits an enhanced mismatch signal compared with the mismatch signal following a short train. This would indicate that a longer and regular train facilitates discrimination of small deviations. We also assessed whether sensitivity to a small DS varies as a function of the number of preceding standard sounds with the linear regression approach. We used trials associated with a deviant stimulus and grouped the trials according to the number of preceding standard sounds. We initially used the 3 levels of lowest DS ( $\leq 150$  Hz) out of the 6 levels of deviations. We used small deviations for 2 reasons. First, finding no amplitude variation could derive from the fact that amplitude variations to large deviations might show a ceiling effect obscuring the gradient as a function of train length. Secondly, if all DSs were collapsed one could argue that small deviations do not have the same impact as large deviations. To prevent this, we tested the influence on small deviations. Note that the same analysis with all 6 levels of DS yielded a comparable result (see [Supplementary Results](#)). As outlined in the section “Coding of the PE”, the evoked

responses of the fourth to the last repetition in a train were designated to the set of standard trials. This results in 7 time series for each subject. Time series were averaged across all recording channels. The individual slope parameters were averaged across participants and the averaged slope parameters were used to determine the temporal intervals in which differences in amplitude predict differences in the number of preceding standards.

#### NAcc–Cortex Interaction

We tested whether the mismatch signal on the level of the NAcc predicts cortical activity by determining trial-by-trial cross-correlation between the NAcc and cortical time series in 2 cortical regions of interest (ROIs). The frontal ROI encompassed Fpz, Fz, and FCz, and the centro-parietal ROI encompassed Pz and Cz. In each trial, the time series were averaged separately across intracranial and surface recording channels leading to 2 time series per trial (intracranial and surface activity). Pearson's correlation  $r$  coefficients were used to quantify the coupling between responses in NAcc and the cortical ROIs. Cross-correlation means that the activity at each time point across trials in the NAcc was correlated with the activity at each time point across trials on the cortical recordings. This provides information about both the strength of correlation and the temporal relation of the correlation. Here, the set of trials designated to the deviant stimuli was used and the same analysis with the set of standard trials revealed no significant interaction between the NAcc and scalp recording sites. We calculated  $r$  values at each sample point ( $N_{\text{comparisons}} = 129 \times 129$ ) and averaged the resulting  $r$ -values across participants. Since  $r$  is not a metric measure before averaging across participants, we transformed  $r$ -values using the inverse hyperbolic tangent in the following equation:

$$\text{atanh}(r) := \frac{1}{2} \ln \left( \frac{1+r}{1-r} \right) \text{ for } |r| < 1.$$

This correlation approach requires statistically independent observations. Statistical significance was assessed by a permutation procedure, which encompasses 500 runs of the same analysis with the same time series but randomly shifted in time and results in CIs for each  $r$ -value. We Bonferroni-corrected for multiple comparisons by dividing the significance threshold by the number of comparisons as follows:

$$P_{\text{corr}} = \frac{0.05}{N_{\text{comparisons}}}.$$

The Bonferroni-corrected  $P$ -value within the empirical distributions was used as the threshold for statistical significance.

## Results

### Deviancy Detection in the NAcc

#### The NAcc Mismatch Signal

We found that between 20 and 130 ms ( $t_4 = -2.9$ ;  $P = 0.001$ ) and between 290 and 410 ms ( $t_4 = 4.1$ ;  $P < 0.0001$ ), the time series for deviant stimuli generated a mismatch signal (Fig. 2A), indicating that the NAcc differentiated between standard and new (deviant) stimuli at these time-epochs. These differences in amplitude were confined to low frequencies (see [Supplementary Material](#) and [Supplementary Fig. 1](#)), being maximal for 11 Hz (range 4–18 Hz) around 240 ms ( $t_4 = 4.866$ ;  $P = 0.004$ ; uncorrected, see [Supplementary Material](#) for differences between temporal intervals in both analyses). In contrast to the NAcc, the ANT does not

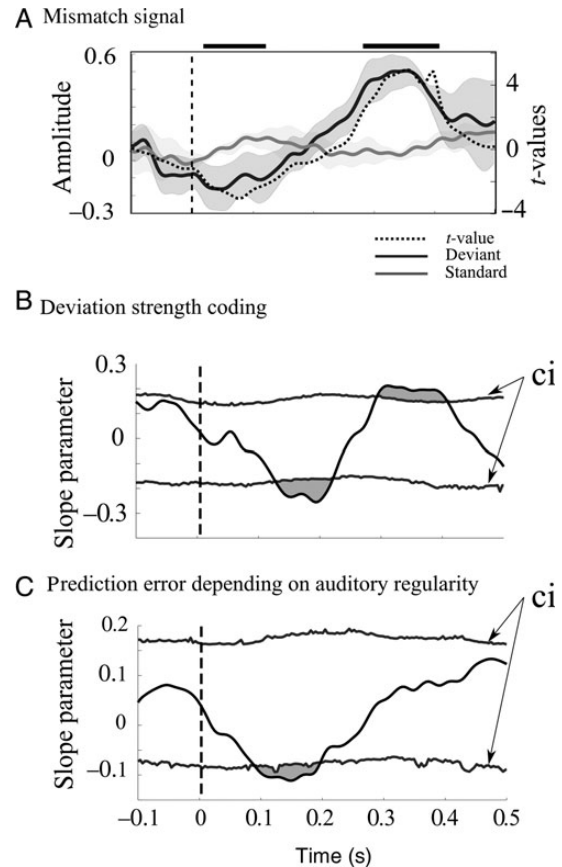


**Figure 2.** In each plot, the vertical dashed line marks the stimulus onset. (A) The NAcc shows a mismatch signal (difference between deviant and standard stimuli) following the presentation of a deviant stimulus. The bold black line gives the mean amplitude for deviant stimuli across participants and the shaded area show the standard error (SE) across participants. The bold gray line shows the mean amplitude for standard trials across participants. The shaded area provides the SE across participants. The left y-axis shows the amplitude values for standard and deviant event-related components. The right y-axis gives the  $t$ -values for the difference between standard and deviant stimuli. The dashed line shows the  $t$ -values as a function of time. The horizontal black bars show the temporal intervals of corrected significant differences. (B) The strength of the deviation (difference in tone pitch between previous standard and the deviant sound) is coded in the NAcc. The amplitude following a deviant stimulus decreases as a function of DS in an early temporal interval and increases gradually later. The black line shows the slope parameter derived from a linear regression at each time point. The curves show the 97.5% and 2.5% CIs derived from a permutation procedure. The gray-shaded areas mark those temporal intervals in which the observed slope parameter underwent or exceeded the empirical distribution. (C) The results presented in B imply that small deviations yield a smaller mismatch signal compared with stronger deviations. We tested whether the amplitude of the mismatch signal to a small DS is modulated by the number of preceding standard trials and hence, auditory regularity. The black line shows the slope parameters as a function of time together with the CIs derived from a permutation procedure. The negative slopes imply that the mismatch signal increases with a negative polarity with an increasing number of preceding standards around 100 ms (gray-shaded area). We tested whether this can be in part due to a repetition suppression within a long train of standards.

differentiate by differences in amplitude between standard and deviant stimuli (see [Supplementary Fig. 2](#)).

#### Activity in the NAcc Represents the Deviation Strength

We then examined whether the NAcc codes for different levels of DS (difference in frequency between the deviant stimulus and

the preceding standard sound). We used all levels of DS ranging from 50 to 300 Hz and predicted the DS from the amplitude value at each time point using linear regression. The observed slope parameters derived from the linear regressions were compared with CIs derived from the permutation procedure. In the time range between 138 and 224 ms ( $P = 0.002$ ) and 302 and 408 ms ( $P = 0.008$ ), the observed slope parameters were significant (Fig. 2B). This indicates that the first significant mismatch signal with a negative polarity linearly codes the DS with a stronger negative amplitude for stronger deviations. The second positive polarity mismatch signal linearly codes the DS with a stronger positive amplitude for stronger deviations.

#### The NAcc Mismatch Signal Depends on the Number of Preceding Standards

To address whether human NAcc responsivity is dependent on the recent past, we evaluated the dependency between the number of prior standard auditory stimuli and the responsivity to a deviant. We hypothesized that sensitivity to deviant stimuli would vary as a function of the number of preceding standard

sounds, where the latter can be thought of in terms of an evolving belief or prior. We tested whether a small DS results in an enhanced amplitude of response as a function of increasing length of a preceding train of standard stimuli. To formally test this, we compared trials with a low DS ( $\leq 150$  Hz) but differing numbers of preceding standard tones. In the time range between 95 and 196 ms ( $P = 0.007$ ), the mismatch elicited a more prominent amplitude following long trains of standards (Fig. 2C). We found a comparable result even when all deviant trials of all levels of DS were subjected to this analysis (see [Supplementary Results](#)). This effect might be explained by repetition suppression (see [Supplementary Material](#)) with an increasing length of preceding trains, but this is unlikely since our test for repetition suppression was not significant (see [Supplementary Fig. 3](#)).

#### Relation of NAcc Activity to the Cortical Response

A cross-correlation revealed that the NAcc trial-to-trial amplitude variation is linked ( $P < P_{\text{corr}}$ ) to the trial-to-trial amplitude variation recorded at centro-parietal, but not frontal, leads. Figure 3 shows that early activity in the NAcc (80–180 ms)

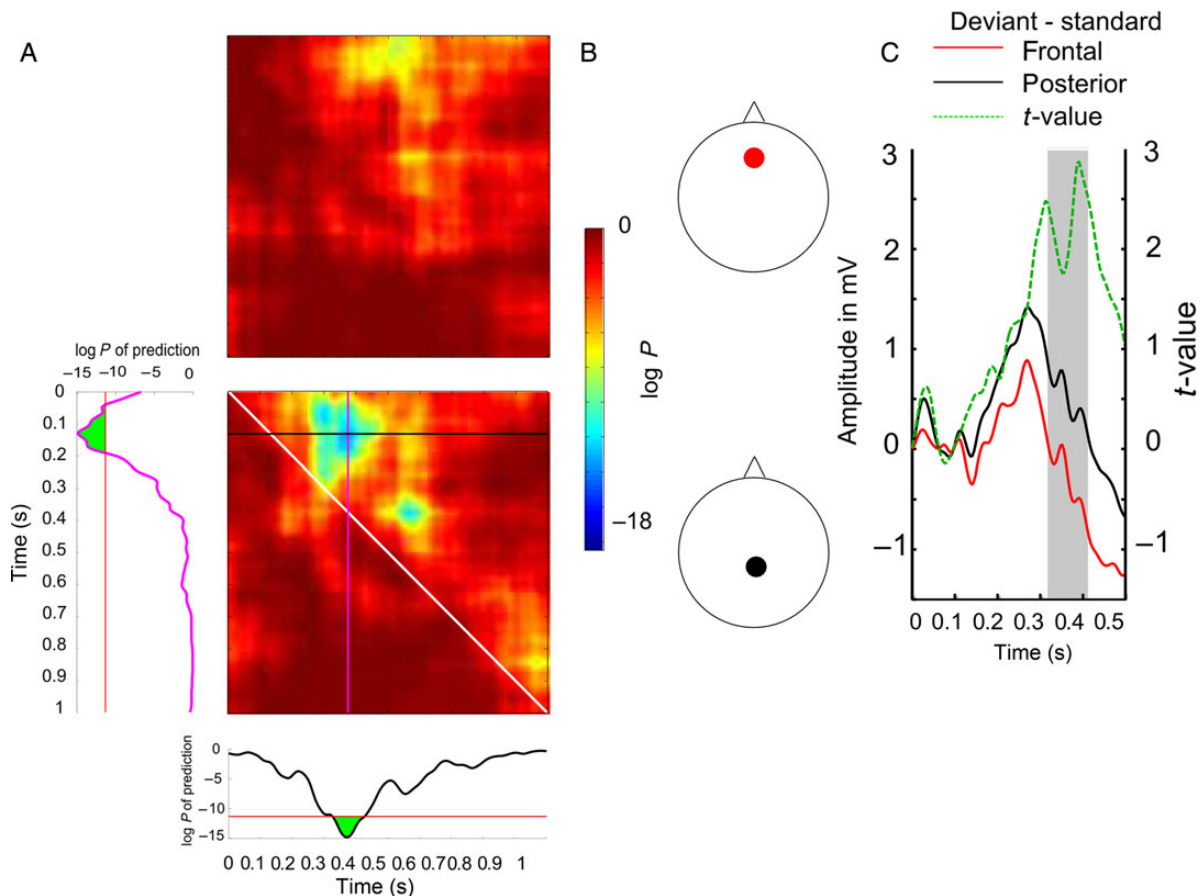


**Figure 3.** Depiction of the cross-correlation analysis. (A) Each point in the upper and lower square matrix shows the correlation strength between the NAcc and the frontal (upper) and the centro-parietal (lower) ROI by means of the probability. The white diagonal separates the direction of temporal relation. All values in the upper triangle show activity in the NAcc preceding surface activity. The lower triangle shows the correlation for surface activity preceding NAcc activity. P-values were derived from a permutation procedure. The strongest correlation as indicated by the smallest P-values is observed between NAcc activity around 120 ms and surface activity around 350 ms. The magenta line shows the correlation of surface activity at around 350 ms with the NAcc at all time points. The black line shows the correlation of NAcc activity at around 120 ms with surface activity at all time points. The red line shows the Bonferroni-corrected significance level. The vertical and horizontal dashed lines mark the beginning of the next trial. (B) The red and black dots show the frontal and centro-parietal ROIs, respectively. (C) Depiction of the difference waves between standard and deviant stimuli within the frontal ROI (red line) and the centro-parietal ROI (black line). Only in the frontal ROI, there is a slight mismatch negativity following 100 ms, which appears to be absent in the centro-parietal potential. The green line gives the t-value for the differences between both ROIs for each time point. In the time range of significant posterior P3 prediction, the frontal and centro-parietal P3 differ significantly.

correlates with activity between 330 and 410 ms at centro-parietal recording sites (maximal  $r = -0.22$ ). Note that the negative correlation coefficient reflects a positive relationship between the amplitude variation at both recording sites. Specifically, the negative correlation results from a correlation between the amplitude of negative deflection in the NAcc and the amplitude of the positive deflection of the P3.

The second positive mismatch signal in the NAcc linearly codes the DS with a stronger positive amplitude for greater deviations. We were unable to establish a scalp correlate of this later NAcc activity. The enhanced early latency NAcc-cortical event related potential correlation was observed for deviation trials, but not for standard trials (see [Supplementary Fig. 4](#)). Note that the frontal P3 was reduced in this time interval relative to the centro-parietal response as is typically observed in paradigms with relatively low stimulus novelty and multiple deviancy repetitions ([Polich 1989a, 1989b; Polich and McIsaac 1994; Fig. 3C](#)). Within the temporal interval of significant prediction, that is NAcc-cortex interaction, the centro-parietal P3 differed significantly from the frontal P3 ( $t_{(4)} = 2.37$ ,  $P = 0.038$ ). Based on these results, we tested for a specific dependency of the posterior P3 amplitude on DS and the number of preceding standards. We conducted the same analysis as described for the NAcc. We found that the posterior, but not the frontal, potential showed a linear dependency on the DS in the time range between 320 and 370 ms ( $P = 0.0065$ ) matching the temporal interval of significant interaction with the NAcc amplitude variation ([Fig. 4A](#)). We also observed that the posterior, but not the frontal scalp, potential showed a linear dependency on the number of preceding standard trials as revealed by statistically significant slope parameters in the time range between 310 and 350 ms ( $P = 0.0031$ ; [Fig. 4B](#)). Moreover, the centro-parietal scalp potential was best predicted by channels located in the central region of the NAcc (see [Supplementary Fig. 5](#)).

## Discussion

We recorded intracranially from the human NAcc using an auditory deviancy paradigm to assess the processing of sensory deviations, allowing us to test whether NAcc contributes to the

computation of statistics in local auditory irregularities. We also determined whether NAcc activity generated to deviant events was linked to a modulation of cortical activity. We observed that human NAcc activity reliably tracks the statistics of the local auditory scene and predicts later cortical activity.

We found that the strength of deviation coded in the NAcc displayed larger responses if they occurred following longer trains of standards. We employed a bipolar montage to insure that the recorded NAcc activity was not due to far-field activity from nearby non-NAcc structures. As a further subcortical control, the anterior thalamic recordings did not signal deviancy from expectancy nor amplitude variation as a function of DS. Thus, the amplitude variation in the NAcc indicates that this activity is dependent on information regarding temporal succession, an effect possibly originating in the hippocampal formation. Indeed, the strong anatomical and functional connection with the hippocampus (HC; [Finch 1996; Goto and Grace 2008](#)) makes the NAcc an ideal structure to track representations of the recent past stored in the HC ([Lisman and Grace 2005](#)), an idea supported by [Strange et al. \(2005\)](#) and [Axmacher et al. \(2010\)](#). [Lisman and Grace \(2005\)](#) proposed a model of novelty detection and memory formation consisting in a functional loop between HC-ventral tegmental area (VTA). This model assumes feedforward and feedback connections. Our NAcc and scalp data in deviation trials provide support for such a functional loop. In contrast, activity evoked by standard stimuli does not influence the late cortical response, suggesting that information about a correct prediction as in the case of a standard trial does not activate the HC-VTA loop.

One question is whether the HC sends information about the quality of deviation or a general signal of deviancy ([Strange et al. 2005](#)). [Dolan and Fletcher \(1997\)](#) showed a functional dissociation between medial temporal and dorsolateral prefrontal (dlPFC) areas during encoding auditory-verbal stimuli, with a medial temporal area more responsive to general novelty and dlPFC responsive to associations between category and exemplars. The present findings support the idea that the NAcc might receive a general novelty signal from the HC. This HC signal might indicate that a PE was committed but not the quality in terms of DS. Support for this interpretation emerges from [Strange et al. \(2005\)](#) who

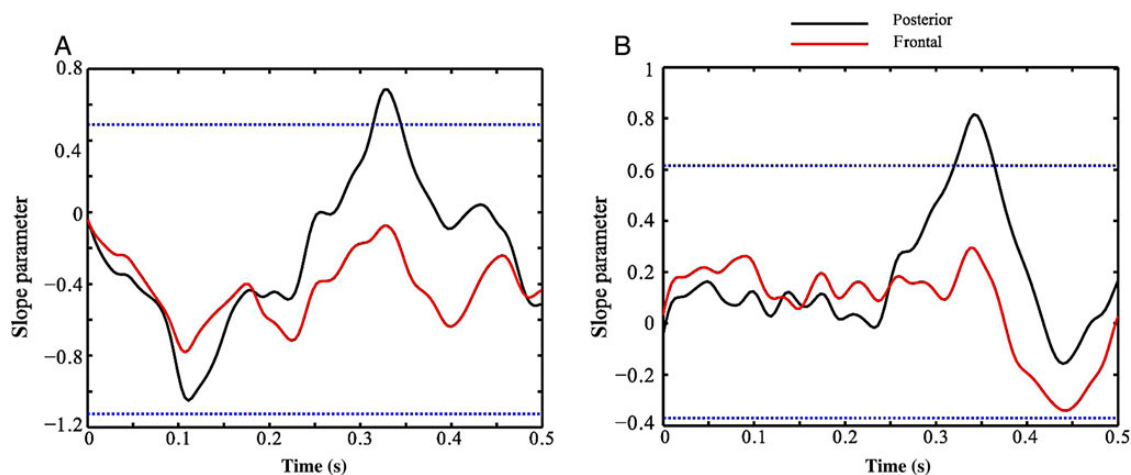


**Figure 4.** (A) The strength of the deviation (difference in tone pitch between previous standard and the deviant sound) is coded in the posterior P3. The amplitude following a deviant stimulus increases as a function of DS in the temporal interval of the P3. The black line shows the slope parameter derived from a linear regression at each time point for the posterior P3, and the gray-dashed line for the frontal P3. The horizontal lines show the 97.5% and 2.5% CIs derived from a permutation procedure. (B) We tested whether the amplitude of the scalp potential modulated by the number of preceding standard trials and hence, auditory regularity. The black line shows the slope parameter derived from a linear regression at each time point for the posterior P3, and the gray-dashed line for the frontal P3. The horizontal lines show the 97.5% and 2.5% CIs derived from a permutation procedure.

showed that the HC response is modulated by entropy. This quantifies expected information rather than the information itself and their study showed that unpredictable stimulus streams led to greater activity in the anterior HC.

We observed the NAcc discriminates deviant events at an earlier latency than previously reported (Axmacher et al. 2010). This might be explained by the simplicity of the stimuli used in our study, and the differences in modality since visual stimuli elicit mismatch-related components with a prolonged latency compared with auditory oddball stimulation (Comerchero and Polich 1999). We speculate that the processing of the visual stimuli called for a cognitive evaluation reducing any automatic early components as observed in the current study. The passive listening in our current study underscores the rapid pre-attentive and automatic process represented in the NAcc signal.

The NAcc is proposed to play a prominent role in goal-directed behavior by integrating inputs from other limbic structures and the prefrontal cortex (Goto and Grace 2008). Since our task design did not require behavioral responses, the influence of detecting local auditory irregularities for directing subsequent behavior cannot be inferred directly. However, the fact that the early mismatch signal in the NAcc selectively correlates with the central-parietal P300 underscores the notion that the NAcc is central to behavioral adjustments. The scalp P300 component is linked to memory storage and detecting behavioral-relevant targets (Knight 1996, 1998; Polich and Criado 2006; Polich 2007). Our study used weak deviants that typically activate only the centro-parietal P300 response to deviant events. This might suggest that contextual deviancy detection occurs in a hippocampal-NAcc network, and this information is used to trigger the activation of a broader attentional network manifested in a scalp P300 potential.

A role for NAcc activity in goal-directed behavior is further supported by differences in the P300 prediction as a function of the subregions of the NAcc assessed in our study. P300 scalp prediction is maximal in central NAcc sites pointing to differences in functional significance of subregions of the human NAcc. In rats, lesions to the NAcc core decreased habituation to a novel environment due to failure in the detection of perturbations (Cardinal et al. 2001). Furthermore, studies in rats show that the core region is involved in inhibitory control of goal-directed behavior (Pothuizen et al. 2005) and is especially necessary for processing of stimuli deviating from expectancy.

Patient intracranial studies carry a possibility of impacting critical processes relevant to mismatch detection and other cognitive functions. All 5 patients were awake, attentive, and responsive during the recording session. Hence, we consider the likelihood of an impact on this automatic process to be relatively small. Furthermore, despite the small number of participants, the effect is strong enough to reliably detect a mismatch signal across subjects.

Taken together, our findings demonstrate that, within an ongoing stream of information, the NAcc contributes to coding the statistics of the auditory environment manifested by a gradual variation of amplitude of the local field potential in the NAcc. This NAcc gradient predicts generation of a subsequent scalp P300 dependent on cortical-hippocampal circuits. These findings emphasize the importance of the NAcc in the automatic integration of sensory information. Furthermore, the relationship between NAcc and the P300 provides evidence for a role of NAcc activity in mnemonic functions possibly by binding neural activity that is shared between medial temporal lobe and dopaminergic midbrain structures.

## Supplementary Material

Supplementary material can be found at: <http://www.cercor.oxfordjournals.org/>.

## Funding

This work was funded by NINDS grant 2R37NS21135, the Nielsen Corporation, Forschungscampus Stimulate, Land Sachsen-Anhalt FKZ I60, Land Sachsen-Anhalt Exzellenzförderung, the Wellcome Trust 091593/Z/10/Z, DFG-SFB 779/TP A2 (T.Z. and H.-J.H.), TP A3 (H.-J.H.) and TP A11 (J.V. and H.-J.H.), DFG He 1531/11-1 (J.V. and H.-J.H.), Federal Ministry of Education and Research (grant no. 03FO16102A) (J.V.), Australian Research Council Discovery Early Career Researcher Award (DE130101393) (M.I.G.), the Australian Research Council Centre of Excellence for Integrative Brain Function (ARC Centre Grant CE140100007) (M.I.G.). This work was supported by the Wellcome Trust (R.J.D Senior Investigator Award 098362/Z/12/Z). The Wellcome Trust Centre for Neuroimaging was supported by core funding from the Wellcome Trust 091593/Z/10/Z.

## Notes

*Conflict of Interest:* None declared.

## References

- Abler B, Walter H, Erk S, Kammerer H, Spitzer M. 2006. Prediction error as a linear function of reward probability is coded in human nucleus accumbens. *Neuroimage*. 31:790–795.
- Axmacher N, Cohen MX, Fell J, Haupt S, Dümpelmann M, Elger CE, Schlaepfer TE, Lenartz D, Sturm V, Ranganath C. 2010. Intracranial EEG correlates of expectancy and memory formation in the human hippocampus and nucleus accumbens. *Neuron*. 65:541–549.
- Baliki MN, Geha PY, Fields HL, Apkarian AV. 2010. Predicting value of pain and analgesia: nucleus accumbens response to noxious stimuli changes in the presence of chronic pain. *Neuron*. 66:149–160.
- Becerra L, Breiter HC, Wise R, Gonzalez RG, Borsook D. 2001. Reward circuitry activation by noxious thermal stimuli. *Neuron*. 32:927–946.
- Blair RC, Karniski W. 1993. An alternative method for significance testing of waveform difference potentials. *Psychophysiology*. 30:518–524.
- Boly M, Garrido MI, Gosseries O, Bruno MA, Boveroux P, Schnakers C, Massimini M, Litvak V, Laureys S, Friston K. 2011. Preserved feedforward but impaired top-down processes in the vegetative state. *Science*. 332:858–862.
- Cardinal RN, Pennicott DR, Sugathapala CL, Robbins TW, Everitt BJ. 2001. Impulsive choice induced in rats by lesions of the nucleus accumbens core. *Science*. 292:2499–2501.
- Comerchero MD, Polich J. 1999. P3a and p3b from typical auditory and visual stimuli. *Clin Neurophysiol*. 110:24–30.
- Dolan RJ, Fletcher PC. 1997. Dissociating prefrontal and hippocampal function in episodic memory encoding. *Nature*. 388:582–585.
- Finch DM. 1996. Neurophysiology of converging synaptic inputs from the rat prefrontal cortex, amygdala, midline thalamus, and hippocampal formation onto single neurons of the caudate/putamen and nucleus accumbens. *Hippocampus*. 6:495–512.

- Garrido MI, Friston KJ, Kiebel SJ, Stephan KE, Baldeweg T, Kilner JM. 2008. The functional anatomy of the MMN: a DCM study of the roving paradigm. *Neuroimage*. 42:936–944.
- Goto Y, Grace AA. 2008. Limbic and cortical information processing in the nucleus accumbens. *Trends Neurosci*. 31:552–558.
- Haenschel C, Vernon DJ, Dwivedi P, Gruzelier JH, Baldeweg T. 2005. Event-related brain potential correlates of human auditory sensory memory-trace formation. *J Neurosci*. 25:10494–10501.
- Kane NM, Curry SH, Butler SR, Cummins BH. 1993. Electrophysiological indicator of awakening from coma. *Lancet*. 341:688.
- Kane NM, Curry SH, Rowlands CA, Manara AR, Lewis T, Moss T, Cummins BH, Butler SR. 1996. Event-related potentials–neurophysiological tools for predicting emergence and early outcome from traumatic coma. *Intensive Care Med*. 22:39–46.
- Knight R. 1996. Contribution of human hippocampal region to novelty detection. *Nature*. 383:256–259.
- Knight RT. 1998. Electrophysiology and behavior converge in human extrastriate cortex. *Nat Neurosci*. 1:546–547.
- Knight RT, Scabini D. 1998. Anatomic bases of event-related potentials and their relationship to novelty detection in humans. *J Clin Neurophysiol*. 15:3–13.
- Kumar S, Sedley W, Nourski KV, Kawasaki H, Oya H, Patterson RD, Howard MA III, Friston KJ, Griffiths TD. 2011. Predictive coding and pitch processing in the auditory cortex. *J Cogn Neurosci*. 23:3084–3094.
- Lisman JE, Grace AA. 2005. The hippocampal-VTA loop: controlling the entry of information into long-term memory. *Neuron*. 46:703–713.
- Polich J. 1989a. Frequency, intensity, and duration as determinants of p300 from auditory stimuli. *J Clin Neurophysiol*. 6:277–286.
- Polich J. 1989b. P300 from a passive auditory paradigm. *Electroencephalogr Clin Neurophysiol*. 74:312–320.
- Polich J. 2007. Updating p300: an integrative theory of p3a and p3b. *Clin Neurophysiol*. 118:2128–2148.
- Polich J, Criado JR. 2006. Neuropsychology and neuropharmacology of p3a and p3b. *Int J Psychophysiol*. 60:172–185.
- Polich J, McIsaac HK. 1994. Comparison of auditory p300 habituation from active and passive conditions. *Int J Psychophysiol*. 17:25–34.
- Pothuizen HHJ, Jongen-Rêlo AL, Feldon J, Yee BK. 2005. Double dissociation of the effects of selective nucleus accumbens core and shell lesions on impulsive-choice behaviour and salience learning in rats. *Eur J Neurosci*. 22:2605–2616.
- Rao RP, Ballard DH. 1999. Predictive coding in the visual cortex: a functional interpretation of some extra-classical receptive-field effects. *Nat Neurosci*. 2:79–87.
- Spicer J, Galvan A, Hare TA, Voss H, Glover G, Casey B. 2007. Sensitivity of the nucleus accumbens to violations in expectation of reward. *Neuroimage*. 34:455–461.
- Strange BA, Duggins A, Penny W, Dolan RJ, Friston KJ. 2005. Information theory, novelty and hippocampal responses: unpredicted or unpredictable? *Neural Netw*. 18:225–230.
- Wood DA, Kosobud AEK, Rebec GV. 2004. Nucleus accumbens single-unit activity in freely behaving male rats during approach to novel and non-novel estrus. *Neurosci Lett*. 368:29–32.
- Zaehle T, Bauch EM, Hinrichs H, Schmitt FC, Voges J, Heinze HJ, Bunzeck N. 2013. Nucleus accumbens activity dissociates different forms of salience: evidence from human intracranial recordings. *J Neurosci*. 33:8764–8771.